Journal of Neuropathology and Experimental Neurology

Vol. 63, No. 4
April, 2004
pp. 338–349

Activation of Matrix Metalloproteinase-3 and Agrin Cleavage in Cerebral Ischemia/Reperfusion

SÒNIA SOLÉ, VALÉRIE PETEGNIEF, ROSER GORINA, ÁNGEL CHAMORRO, AND ANNA M. PLANAS

Abstract. Matrix metalloproteinase-3 (MMP-3) degrades components of the extracellular matrix and may participate in the pathogenesis of stroke. Here we examine the expression, activation, and cellular location of MMP-3 and the cleavage of agrin, an MMP-3 substrate, following transient middle cerebral artery occlusion in the rat. MMP-3 was activated by ischemia/reperfusion, which was revealed by the appearance of a cleaved form and increased degradation of a substrate. MMP-3 was observed in ischemic neurons, oligodendrocytes, microvasculature, and reactive microglia/macrophages. In cell cultures, MMP-3 expression was observed in neurons and, to a lesser extent, in mature oligodendrocytes, but not in oligodendrocyte progenitors, astrocytes, or microglia. Casein zymography revealed MMP-3 in cultured neurons. Agrin was expressed in cultured neurons and cultured astrocytes. In brain tissue, agrin was detected in neurons, and following ischemia it was also detected in reactive astrocytes. Addition of MMP-3 to protein extracts from control brain caused neuronal agrin degradation. Following ischemia/reperfusion, agrin disappeared from the tissue membrane fraction and a cleaved agrin fragment was found in tissue protein extracts. The present results show MMP-3 activation and neuronal transmembrane agrin cleavage after ischemia/reperfusion. In addition, the finding that MMP-3 cleaves brain agrin strongly suggests that ischemia-induced MMP-3 activation causes agrin cleavage.

Key Words: Agrin; Ischemia/Reperfusion; Matrix metalloproteinase.

INTRODUCTION

Matrix metalloproteinase-3 (MMP-3), also named stromelysin-1, degrades a wide range of components of the extracellular matrix (1) and is involved in pathologies of the nervous system. In glial tumors, it is responsible for the invasive properties of astrocytoma cells (2). MMP-3 is upregulated prior to the onset of demyelinating diseases (3), it is associated with white matter damage in vascular dementia (4) and it seems to be involved in ischemic neuronal death (5). MMP-3 is expressed as a 57/59 kDa prozymogen; activation of the MMP family of proenzymes occurs following the cleavage of a coordination bond between a zinc ion at the active center and an unpaired cysteine in the aminoterminal propeptide, which can occur following a proteolytic or a chemical bond rupture (6). However, for MMP-3, disruption of the cysteine-75 and zinc ion coordination is not sufficient to activate the precursor protein, as conformational changes in pro-MMP-3 accompanied by the proteolytic cleavage of the cysteine-containing propeptide domain are necessary for the expression of proteolytic activity (7). This proteolytic cleavage, which seems to be essential for MMP-3 activation, results in the conversion of the pro-form to lower molecular weight active forms (45, 28, and 21 kDa).

Matrix substrates for MMP-3 include fibronectin, laminin, elastin, collagen IV, proteoglycans (8, 9), the glycoprotein osteopontin (10), and the cellular matrix protein SPARC (11). In addition to cleaving matrix proteins, MMP-3 degrades other substrates and has been reported to degrade myelin basic protein (12), to cleave intact IgG to produce a single chain Fc-like fragment (13), and to activate MMP-9 in human breast carcinoma cells (14). In addition to the devastating action of MMP-3 on a large spectrum of substrates, it might also have a beneficial anti-inflammatory role due to its ability to cleave all monocyte chemoattractant protein chemokines, generating CC chemokine receptor antagonists (15). MMP-3 also degrades agrin (16), a heparan sulfate proteoglycan (17), which is a component of the synaptic basal lamina at the neuromuscular junction (18). Following release by motoneurons, agrin has the ability to induce clustering of acetylcholine receptors on cultured myotubules (19). A shorter agrin isoform is expressed in the brain, where it remains bound to various types of neuronal cells (20), and is not restricted to cholinergic regions (21). A distinct promoter drives the expression of the neuronal form of agrin (22). Agrin is tightly associated, but not covalently bound (23), with axonal and synaptic membranes of neurons (23–25). Agrin derived from central nervous system basal lamina is functionally different from the agrin isoforms at the neuromuscular junction, as the former does not induce acetylcholine receptor aggregation on cultured myotubes (23). Although brain agrin function is not fully understood (26), several lines of evidence suggest that it can mediate transynaptic signaling (27) and that it regulates neuronal responses to excitatory neurotransmitters, as mice and cultured cortical neurons deficient in agrin are resistant to excitotoxic insults (28).

Ischemia causes early disturbances to the white matter and axons resulting in impaired synaptic transmission (29). As brain agrin has been attributed a putative function at the CNS synaptic cleft, agrin degradation might

From Departament de Farmacologia i Toxicologia (SS, RG, AMP), IIBB-CSIC, and Institut de Malalties del Sistema Nerviós (AC), Hospital Clínic, Institut d'Investigacions Biomèdiques August Pi i Sunyer (IDIBAPS), Barcelona, Spain.

Correspondence to: Dr. Anna M. Planas, Departament de Farmacologia i Toxicologia, IIBB-CSIC, IDIBAPS, Rosselló, 161, planta 6, 08036, Barcelona, Spain. E-mail: ampfat@iibb.csic.es

This study was supported by a grant from the Spanish Ministry of Science and Technology (MCYT, SAF2002-01963).

contribute to functional alterations following cerebral ischemia. A recent genomic study of the ischemic rat brain showed reduced expression of agrin mRNA (30), but whether agrin protein is modified after ischemia has not been explored. Active MMP-3 is a candidate to cause agrin cleavage in ischemia. MMP-3 expression has been shown in the ischemic brain (5), but MMP-3 activation following ischemia has not been demonstrated. Here we address the question of whether MMP-3 is activated in the rat brain following ischemia/reperfusion, and whether agrin is subsequently degraded.

MATERIALS AND METHODS

Animals and Surgery

Adult male Sprague-Dawley rats (275–325 g body weight; n = 50) obtained from Iffa-Credo (Lyon, France) were kept under a 12-hour light-dark cycle and allowed free access to food and water. Animal work was conducted in compliance with the Spanish legislation on ''Protection of Animals used for Experimenting or other Scientific Purposes'' and in accordance with the Directives of the European Community. Rats were initially anesthetized with 4% halothane in a mixture of 70% N_2O and 30% O_2, and after tracheal intubation for controlled ventilation, anesthesia was maintained with 1% to 1.5% halothane. The left femoral artery was cannulated for monitoring blood pressure and body temperature was maintained at 36.5 to 37.5°C with a heating blanket connected to a rectal probe. Transient focal cerebral ischemia was induced by middle cerebral artery (MCA) occlusion using an intraluminal technique, as reported previously (31). Briefly, the right MCA was occluded by introducing a 26-mm-long, 3/0 nylon monofilament, blunted at the tip, through the internal carotid artery to the level where the MCA branches out. Both common carotid arteries were clamped to minimize collateral circulation (32). After 50 min, the clip on the left common carotid artery was removed and 10 min later the filament was withdrawn and the clip on the right common carotid artery was also removed. Following surgery, rats were allowed to recover spontaneous breathing. Finally, rats were killed under halothane anesthesia at 4 hours, 1, 4, 7, and 14 days after the onset of reperfusion. For control purposes the left ipsilateral hemisphere of all the rats subjected to ischemia/reperfusion was used, and in addition, the brains of nonoperated rats (n = 6) were also studied. Note: these rats were anesthetized before killing according to the ethical procedures of our institution.

Primary Cell Culture Preparation

Neuron-enriched cultures were prepared from embryonic day 18 (E18) Sprague-Dawley rats (Iffa-Credo) as previously described (33), with modifications. Reagents, unless otherwise stated, were from Invitrogen (Paisley, Scotland, UK). Cells were resuspended in modified Eagle's medium (MEM) (Sigma-Aldrich, Alcobendas, Spain) supplemented with 10% fetal calf serum and 100 μg ml^{-1} gentamycin and seeded at a density of 3,680 cells/mm^2. Six μM cytosine arabinose was added after 4 days in vitro. At 7 and 10 days in vitro, part of the medium was replaced with MEM containing B27 supplements with 3 μM cytosine arabinose to prevent proliferation of non-neuronal cells.

Glial cell cultures enriched in astrocytes were prepared from the cerebral cortex of P1-P2 postnatal Sprague-Dawley rats as previously described (34), with slight modifications. Cells were plated and maintained in Dulbecco's modified Eagle medium (DMEM, Gibco-BRL, Invitrogen, Paisley, UK) supplemented with 20% fetal bovine serum (FBS) (Gibco-BRL). The culture medium was changed twice per week. After 1 week, the flasks were shaken at 200 rpm for 2 hours to dislodge microglia. The medium was removed and replaced with fresh medium containing 10% FBS. Subsequently, until the cells reached confluence, 7% FBS was used in the medium.

Microglial cultures were prepared from cultures of rat primary mixed glia at 7 to 8 days in vitro by shaking the cells for 2 hours at 200 rpm, as reported elsewhere (35). Floating cells were collected and sub-cultured at 5×10^4 cells ml^{-1} and maintained with the tissue medium as above, containing 7% FBS.

Oligodendrocyte cultures from rat brain were provided by Dr. Eduardo Molina-Holgado and were prepared as described elsewhere (36). Oligodendrocyte progenitors were grown in culture for 3 days in serum-free medium containing 2.5 ng ml^{-1} basic fibroblast growth factor and human recombinant platelet-derived growth factor-α (PreproTech Inc., Rocky Hill, NJ), which expanded the number of cells while preventing differentiation by maintaining the cells as a population of homogeneous bipolar cells. Mature oligodendrocytes were obtained by further culturing the cells for up to 10 days in the same medium as above, supplemented with 3% calf serum (Gibco-BRL). These cells acquired a complex morphology with ramified processes.

Protein Expression by Western Blotting

Cell culture and tissue samples were homogenized in radioimmunoprecipitation assay lysis buffer with a protease inhibitor cocktail (Boehringer Mannheim, Mannheim, Germany), as reported previously (34). Samples were sonicated and then centrifuged at 12,000 × *g* for 15 min at 4°C, and the supernatants were used as the protein fraction. The protein content was determined with the Bradford assay (Bio-Rad, Hercules, CA). A different set of frozen tissue samples from control and ischemic brains was used to obtain the cytosolic membrane protein fraction using a sucrose gradient method, as previously reported (37). Each sample (controls, n = 3; ischemic, n = 3) was obtained by pooling frozen brain tissue from 2 rats. Briefly, tissue was homogenized with a loose Dounce homogeniser in buffer (1:3 w/v) containing 1 mM $NaHCO_3$ and 0.5 mM $CaCl_2$, pH 7.5. The homogenate was filtered and centrifuged at 1,000 × *g* for 20 min. The pellet was resuspended in the same buffer and centrifuged at 1,500 × *g* twice for 15 min each, then resuspended and centrifuged at 1,550 × *g*. The pellet was then resuspended in 80% sucrose to a final volume of 10 ml and homogenized with a tight Dounce homogenizer. Then, a sucrose gradient (solutions were made in 5 mM tris-HCl buffer, pH 7.5) was prepared by sequentially adding 8 ml 80% sucrose, 8 ml 48% sucrose, 8 ml 47% sucrose, and 6 ml 41% sucrose, which was subjected to ultracentrifugation at 90,000 × *g* for 2 hours. The membrane enriched fraction (found between 47%–41% sucrose) was centrifuged at 100,000 × *g* for 30 min in 10 mM Tris-HCl buffer pH 7.4 containing 3 mM EGTA. Finally, the

pellet was resuspended in the last buffer and the protein content was determined as above.

Protein samples were run alongside prestained molecular weight markers (Bio-Rad) in denaturing 6% to 8% polyacrylamide gels and were transferred to a membrane (Immobilon-P, Millipore, Bedford, MA), as reported previously (34). Membranes were incubated overnight at 4°C with one of the following primary antibodies: mouse monoclonal antibodies against rat Agrin (Agr-520, StressGen, Victoria, Canada) diluted 1:250, β-tubulin (Boehringer Mannheim) diluted 1:5,000, synaptophysin (clone SY 38, Dako, Glostrup, Denmark) diluted 1:7,000, ED1 (MCA341, Serotec, Kidlington, Oxford, UK) diluted 1:300; and rabbit polyclonal antibodies against the MMP-3 hinge region (M4802, Sigma) diluted 1:1,000, actin (Sigma) diluted 1:5,000, MMP-2 (AB809, Chemicon, Temecula, CA) diluted 1:2,000, glial fibrillary acidic protein (GFAP, Dako) diluted 1:1,000. The secondary antibodies (Amersham, Piscataway, NJ) were peroxidase-linked anti-mouse Ig or anti-rabbit Ig diluted 1:2,000. The reaction was developed with a chemiluminescence reagent containing luminol. Densitometric analysis of band intensity in the blots was carried out with a Kodak camera (DC-120) and Kds1D Digital Science System software.

Enzymatic Assay of MMP-3 Activity

MMP-3 activity was assessed by incubation of control and ischemic brain samples with a fluorogenic substrate (MMP-3 Substrate II, Calbiochem, San Diego, CA), which is degraded by MMP-3 (38). Frozen tissue was homogenized in lysis buffer containing 50 mM Tris-HCl pH 7.6, 150 mM NaCl, 5 mM $CaCl_2$, 0.05% Brij-35, 0.02% NaN_3, and 1% Triton X-100, and centrifuged at 12,000 × *g* for 5 min at 4°C. The supernatants, containing 200 μg of protein (in a volume of 50 μl), were mixed with assay buffer (50 mM Tris-HCl pH 7.6, 200 mM NaCl, 5 mM $CaCl_2$, 20 μM $ZnSO_4$ and 0.05% Brij-35) to a final volume of 200 μl, and different concentrations of the fluorogenic MMP-3 substrate (1, 2.5, 5, 10, and 30 μM) were added. The samples were incubated for 10 min at 37°C and fluorescence was measured on a fluorimeter (Spectra Max GeminiXS, Molecular Device Corporation, Sunnyvale, CA) (λ_{exc} = 328 nm and λ_{em} = 393 nm). A mixture of lysis buffer with assay buffer in the absence of tissue samples was incubated as above as a reaction blank. Data was analyzed by nonlinear regression and fitted to one-phase exponential association curves. The rate constant and the Y_{max} values were calculated and statistical comparisons between rat groups were performed with the unpaired *t*-test.

Immunohistochemistry and Histochemical Reactions

Rats were perfused with 4% paraformaldehyde and brains were postfixed overnight with the same fixative and then embedded in paraffin. Five-μm-thick coronal sections were obtained with a microtome. Studies were performed 1, 4, 7, and 14 days after ischemia and in controls (n = 3 per group). Paraffin was removed and sections were boiled in 10 mM citrate buffer, pH 6, for 20 min for antigen retrieval. Immunohistochemistry was carried out as previously reported (37). Endogenous peroxidases were blocked with methanol-H_2O_2, and *non*-specific-binding sites with 3% normal horse or goat serum for 2 hours. Sections were then incubated overnight in a humidified chamber at 4°C with either the mouse monoclonal antibody against CNS agrin (agr-520) diluted 1:25, a mouse monoclonal antibody against GFAP (Boehringer Mannheim) diluted 1:500, or a rabbit polyclonal antibody against MMP-3 (Sigma) diluted 1:200. Sections were incubated with biotinylated horse anti-mouse or goat anti-rabbit IgG (Vectastain, Vector, Burlingame, CA) diluted 1:200 for 1 hour and then avidin-biotin-peroxidase (ABC kit, Vector) (1:100) for 1 hour. The reaction was developed with 0.05% diaminobenzidine and 0.03% H_2O_2. Immunoreaction controls included omission of the primary antibody. Several sections were counterstained with hematoxylin. Double immunohistochemistry (37) was performed after the first immunoreactions. Sections previously reacted with the first primary antibody were incubated overnight with the second primary antibody, followed by a biotinylated secondary antibody. Then the sections were incubated with the avidin-biotin complex, washed with 0.01 M sodium phosphate buffer, pH 6, and preincubated for 10 min with 0.01% benzidine dihydrochloride and 0.025% sodium nitroferricyanide in 0.01 M sodium phosphate buffer, pH 6. The reaction was developed in this solution with 0.005% H_2O_2.

Lectin histochemistry to label microglia/macrophages was carried out by incubating the section with biotinylated lectin from Lycopersicon esculentum (Sigma), as reported previously (37), following incubation with the primary antibody. For control purposes, we carried out the same double histochemistry procedures in the absence of either the first primary antibody or the lectin.

For Luxol fast blue (Klüver-Barrera) staining, sections were immersed in 95% ethanol and were stained in a Luxol fast blue solution (0.1% in 95% ethanol) for 2 hours at 60°C, and the excess stain was rinsed with 95% ethanol. The sections were rinsed with distilled water and differentiated the staining by immersion in a 0.05% lithium carbonate solution for 30 seconds. We continued differentiation in the 70% ethyl alcohol and when differentiation was completed (i.e. grey and white matter was visually distinguished), we washed in distilled water, dehydrated the sections, and mounted the preparations.

Casein Zymography in Cultured Cells

Zymography was performed in 8% polyacrylamide gels containing casein (1 mg ml^{-1}). The casein solution (from bovine milk, Sigma) (10 mg ml^{-1}) was prepared by mixing with 1.5 M Tris-HCl pH 8.8 for 2 hours under vortex shaking. Ten μg of protein was loaded in the gel and SDS-PAGE was performed at 100 V. The gels were incubated in 250 ml of buffer containing 50 mM Tris-HCl pH 7.5, 10 mM $CaCl_2$ and 0.02% NaN_3 for 42 hours at 37°C. Incubation in the presence of 20 mM EDTA was carried out as a control for the specificity of the caseinolytic reaction. After incubation, gels were stained in 0.1% amido black (napthol blue black, Sigma) in acetic acid: methanol:water (1:3:6) for 30 min and washed in the solvent 4 times for 15 min each, followed by a final wash in distilled water.

Agrin Degradation by MMP-3

The tissue homogenates (as used for Western blot, described above) containing 300 μg of protein in approximately 30 μl were mixed to a final volume of 200 μl with incubation buffer

containing 50 mM Tris-HCl pH 7.5, 10 mM $CaCl_2$, and 0.02% NaN_3, and in the presence or absence of 500 U of human recombinant MMP-3 (catalytic domain, from Calbiochem) (1.6 U/μg of protein). Incubation was carried out for 18 hours at room temperature under constant shaking. Forty μg of protein was denatured and loaded on a 6% polyacrylamide gel for Western blot analysis of agrin.

RESULTS

Expression of MMP-3

Basal expression of MMP-3 pro-form in control brain tissue was detected by Western blot analysis as a band of ~57 kDa (Fig. 1A). A faint band of ~120 kDa, which might correspond to MMP-3 dimers, was detected in the blots, but no changes were seen in the intensity of this band after ischemia/reperfusion (Fig. 1A). However, ischemia/reperfusion caused the appearance of an additional band of lower molecular weight (45 kDa, n = 12), which corresponds to an active form of MMP-3 at 1, 4, and 7 days post-ischemia, but not at 4 hours (Fig. 1A). Quantification of the intensity of this band by densitometric analysis showed a significant ($p < 0.001$) increase at 1, 4, and 7 days after ischemia/reperfusion (Fig. 1B).

MMP-3 Activity in Brain Tissue after Ischemia

We determined the extent to which brain tissue samples were able to degrade a specific MMP-3 fluorogenic substrate, which becomes fluorescent following cleavage. We measured the fluorescence (excitation = 368 nm, emission = 459 nm) after addition of various substrate concentrations ranging from 0 to 30 μM. Data for each group of rats (4–6 rats per group) was obtained after 10-min incubation and fitted to a curve by means of *non*linear regression (1 phase exponential association) (Fig. 1B). The control group fitted with $R^2 = 0.998$, the 1-day post-ischemia experiment group fitted $R^2 = 0.996$, and the 4-day group fitted $R^2 = 0.997$. Mean ± SEM values for the rate constant (K) were 0.121 ± 0.011 for controls, while the corresponding values for 1 day and 4 days post-ischemia were 0.206 ± 0.039 and 0.1817 ± 0.020, respectively. The higher K value (Fig. 1C) after ischemia ($p < 0.05$) is compatible with an increase in the activity of MMP-3. Y_{max} values were 1,298 ± 63 for controls and 1,189 ± 105 and 1,843 ± 92 for 1 and 4 days post-ischemia, respectively. The Y_{max} value can be taken as the capacity of the enzyme to bind substrate, suggesting an increased MMP-3 protein expression by 4 days post-ischemia ($p < 0.001$) (Fig. 1C). At this time point, expression of MMP-3 was found in reactive microglia/macrophages (Fig. 2S), indicating that there was more enzyme present in the tissue for binding its substrate.

Cellular Localization of MMP-3

We detected expression of MMP-3 in the control brain (Fig. 2A, I, N), mainly localized in neurons as evidenced in Figure 2N by double immunostaining with NeuN, which is a marker of neuronal nuclei. Neurons showed faintly stained cytoplasm and processes, and a discrete granular staining in their nucleus. In addition, MMP-3-stained oligodendrocytes were detected in the control white matter as shown in Figure 2E (light brown) and Figure 2G (dark brown). Double immunohistochemistry with GFAP revealed no stained astrocytes (Fig. 2A, E). Likewise, no MMP-3 staining was detected in resting microglia, or the microvasculature (Fig. 2A, arrowhead).

At 24 hours of reperfusion after 1-hour MCA occlusion, increased MMP-3 staining was detected in neurons located in the periphery of the ischemic core (Fig. 2B). Within the ischemic core there were many MMP-3-stained neurons showing a typical morphology of ischemic neurons with a triangular shape and a very shrunken nucleus that was immunoreactive to MMP-3 (Fig. 2C, J, L). In this area, stained processes were no longer seen and, besides the stained neurons, the overall immunoreactivity was reduced compared with that in the contralateral hemisphere (Fig. 2C). At this time, MMP-3 staining was prominent in oligodendrocytes located in the ipsilateral white matter (Fig. 2F). MMP-3 staining in oligodendrocytes of the white matter was very intense by 4 days post-ischemia (Fig. 2H). At this time, disrupted myelin fibers were detected in the ipsilateral corpus callosum after Luxol fast blue staining (bright blue patch in Fig. 2H). Also, by 4 to 7 days post-ischemia, lectin-positive (Fig. 2Q) reactive microglia/macrophages within the infarcted core were immunoreactive to MMP-3 (Fig. 2S), and again no MMP-3 was detected in reactive astrocytes (not shown). At 14 days, the intense staining of oligodendrocytes and microglia/macrophages in the ipsilateral hemisphere was maintained and certain neurons in the periphery of the infarcted core showed intense staining, which became apparent even in the nucleus (not shown). In addition, we observed an increased MMP-3 staining in the microvasculature at 1 day (Fig. 2D, F) and 4 days (Fig. 2S) post-ischemia.

As MMP-3 was reported in astrocytes under certain conditions (39), we decided to separately culture different neural cell types to study MMP-3 expression. We studied primary cultures of rat astrocytes, neurons, microglia, and oligodendrocytes. Markers of the different cell types were used to illustrate the enrichment of each culture in each particular cell type (Fig. 1E). In agreement with data obtained from brain tissue, the results in cultured cells (Fig. 1E) revealed expression of MMP-3 in neurons (Fig. 1E, lanes 1 and 2) and mature oligodendrocytes (Fig. 1E, lane 8), but not in oligodendrocyte precursors (Fig. 1E, lane 7), astrocytes (Fig. 1E, lanes 5 and 6), or microglial cells (Fig. 1E, lanes 3 and 4). Casein zymography in extracts of the different cell types showed MMP-3 activity in neurons (Fig. 1F). The intensity of the neuronal zymography

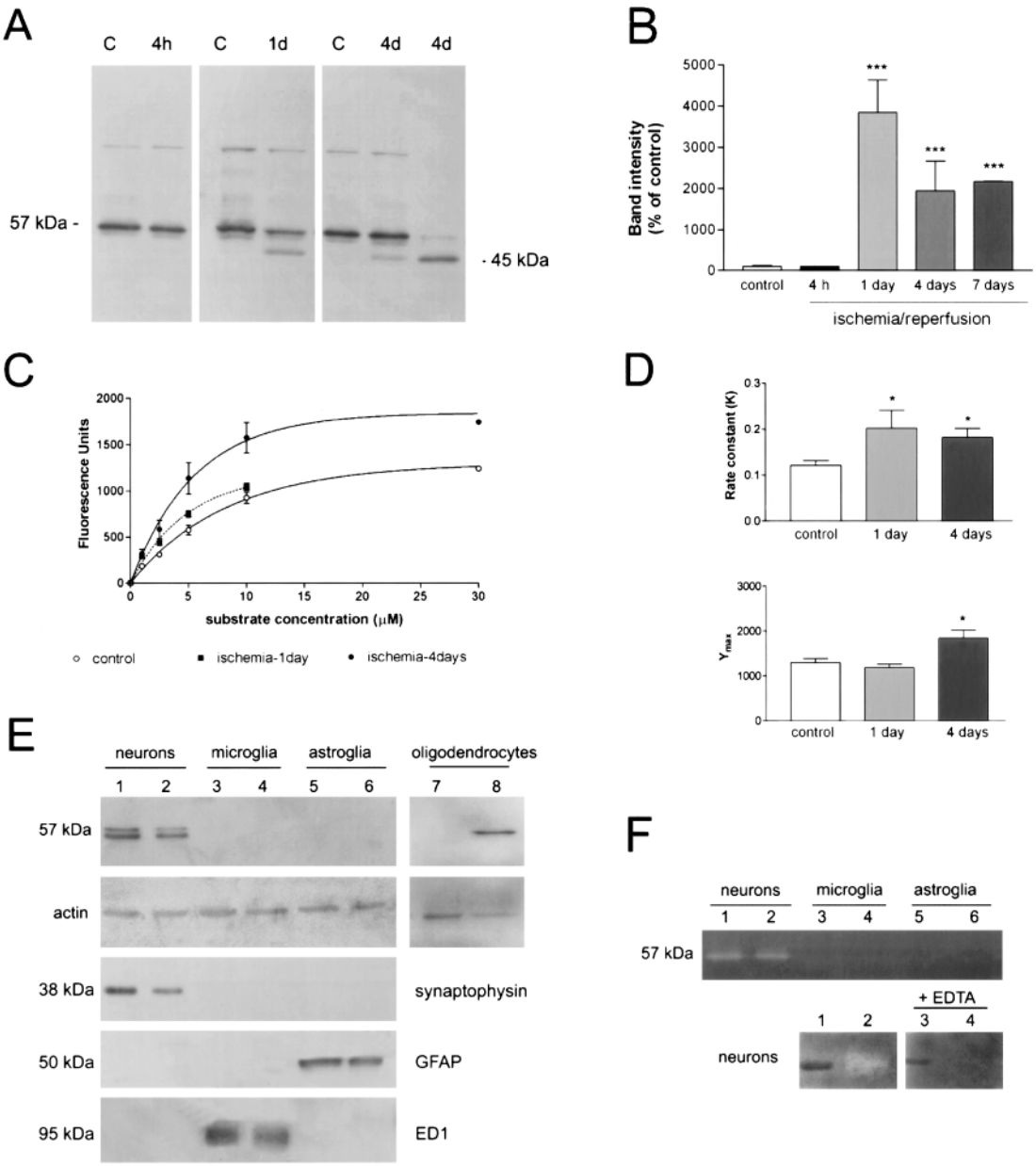

Fig. 1. MMP-3 is activated in the rat brain following MCA occlusion/reperfusion and is expressed in neurons and mature oligodendrocytes in cell cultures, but not in astroglia or microglia. **A:** A 57-kDa precursor form of MMP-3 is expressed in the control brain (from rats not subjected to ischemia and in the contralateral hemisphere of ischemic rats). At 1 and 4 days after the onset of ischemia, but not at 4 hours, a 45-kDa band corresponding to an active form of MMP-3 is found. This is accompanied with some loss of the prozymogen, which is more apparent at 4 days. **B:** Densitometric analysis of the intensity of the 45-kDa band shows a significant (*** indicates $p < 0.001$, *t*-test) increase at 1 day (n = 7), 4 days (n = 3), and 7 days (n = 2) following MCA occlusion in relation to controls (n = 10). Values are expressed as the percentage of control. **C:** Homogenates of brain tissue (n = 4 to 6 rats in each group: controls, 1 day and 4 days ischemia) were incubated in vitro for 10 min with an MMP-3 substrate that emits fluorescence once it has been cleaved by the enzyme (see Materials and Methods). We measured the fluorescence (excitation = 368 nm, emission = 459 nm) that was produced using several substrate concentrations ranging from 0 to 30 μM. Points were fitted to 1-phase exponential association curves using *non*linear regression analysis and the rate constant and Y_{max} parameters were estimated. **D:** The rate constant was higher in both ischemic groups than in the control, indicating a higher activity of the enzyme, whereas the Y_{max} value was higher only at 4 days post-ischemia, compatible with a higher binding capacity in this group (* indicates $p < 0.05$ using the unpaired *t*-test assay). **E:** In cell cultures, the precursor form of MMP-3 was found in cultured neurons (lanes 1, 2) and mature oligodendrocytes (lane 8), but not in precursor oligodendrocytes (lane 7), microglia (lanes 3, 4), or astroglia (lanes 5, 6). Actin is shown as a control for protein loading. Synaptophysin, GFAP, and ED1 blots are shown to identify neurons, astrocytes, and microglia, respectively. **F:** Casein zymography revealed the presence of a band in neurons (lanes 1, 2) but not in microglia (lanes 3, 4) or astroglia (lanes 5, 6). In the bottom part of the figure, casein zymographies

band was attenuated when incubation for casein degradation was performed in the presence of 20 mM EDTA, which inhibits Ca^{2+}-dependent MMP-3 activity (Fig. 1F, bottom gels).

MMP-3 Degrades Brain Agrin and Agrin Is Degraded following Ischemia/Reperfusion

We incubated extracts of control brain in the presence or absence of MMP-3 for 18 hours at room temperature. MMP-3 caused agrin degradation of the full transmembrane agrin form of 220 kDa, as revealed by Western blot (Fig. 3A). Likewise, ischemia/reperfusion caused transmembrane agrin cleavage, as a reduction of the 220-kDa band was detected in membrane extracts (Fig. 3B). In whole brain protein homogenates, attenuation of the intensity of the 220-kDa band after ischemia/reperfusion (at 1, 4, and 7 days) was accompanied by the formation of a lower molecular weight band (135 kDa) (Fig. 3C). The low molecular weight band seen in the total protein extracts of the ischemic brains was not detected in the membrane extracts of ischemic brains (Fig. 3B), demonstrating that the cleaved form of agrin did not remain attached to the membrane. The cleaved fragment of agrin that we detected here contains the C-terminal domain, as the antibody used recognized an epitope located close to the C-terminus of agrin forms containing inserts at splicing site Z; expression of these forms is restricted to the brain.

Cellular Localization of Agrin

We studied agrin expression in primary cultures of neurons, astrocytes, microglia, and oligodendrocytes. Agrin was detected in cultured neurons, and to a lesser extent cultured astrocytes, but not in oligodendrocytes or microglia (Fig. 3D).

Low agrin expression was found in the control rat brain tissue by immunohistochemistry and staining was located in neurons (Fig. 4A). Staining was localized in neuronal processes and around the cell bodies, which is compatible with the presence of agrin in the cell membrane. At 24 hours post-ischemia, agrin staining faded away within the ischemic core (Fig. 4C). However, in the vicinity of the ischemic core, in a penumbra-like area surrounding the core, the intensity of staining was increased around the cell bodies of scattered neurons (Fig. 4B). Here the pattern of agrin staining in neuronal fibers changed, as some parts of neuronal processes showed a higher intensity of staining (Fig. 4B), which might reflect disturbances in agrin trafficking from cell bodies to the synaptic terminals. By 4 to 7 days after MCA occlusion, agrin staining was found in reactive astrocytes forming the glial scar around the infarcted core (Fig. 4D, E) and in extracellular deposits in the vicinity of blood vessels (Fig. 4H). Within the infarcted core, strong staining was observed in granulated deposits inside reactive microglia/macrophages (Fig. 4F). Formation of the agrin-positive granules progressed with time, as they became more intensely stained and showed a more compacted appearance by 14 days post-ischemia (Fig. 4I).

DISCUSSION

MMP-3 in Neurons of the Ischemic Brain

We demonstrated activation of MMP-3 in cerebral ischemia/reperfusion by the appearance of an active band of 45 kDa that was not present in the control brain. MMP-3 expression after ischemia has previously been shown in ischemic neurons and microglial cells at 24 hours following transient MCA occlusion in rats (5). In agreement with this study, we found strong expression of MMP-3 in ischemic neurons in the core showing a typical triangular morphology, which is compatible with a process of ischemic cell death (39). Thus, besides its extracellular role in degrading matrix components, it is likely that neuronal MMP-3 becomes active inside the cells and acts as a proteolytic enzyme degrading cellular components during ischemic cell death. This does not necessarily imply that MMP-3 is involved in causing cell death, as it might simply be a consequence of the cell death process.

MMP-3 Cleaves Transmembrane Neuronal Agrin

We have shown that MMP-3 degrades brain agrin, which is located in neurons, and we observed the disappearance of neuronal agrin from cell membranes after ischemia. Concomitantly, we found an agrin fragment of lower molecular weight that did not remain associated with the membranes, suggesting the release of cleaved agrin to the parenchyma. Agrin removal from the synaptic basal lamina by MMP-3 has been shown at the neuromuscular junction (16) for this agrin isoform, named LN form, but it has not been previously described for the brain agrin isoform, named SN form (20). Although these 2 agrin isoforms are derived from the same gene, they correspond to proteins with different NH_2 termini that differ in their subcellular location, tissue distribution, and function (20). Both isoforms are externalized from cells, but whereas LN agrin assembles into the basal lamina,

←

are shown for aliquots of the same neuronal culture (lanes 2 and 4). Lanes 1 and 3 show a prestained molecular weight marker (50 kDa). The gel on the left side was incubated in the absence of EDTA, whereas the gel on the right side was incubated in the presence of 20 mM EDTA, which inhibits MMP-3.

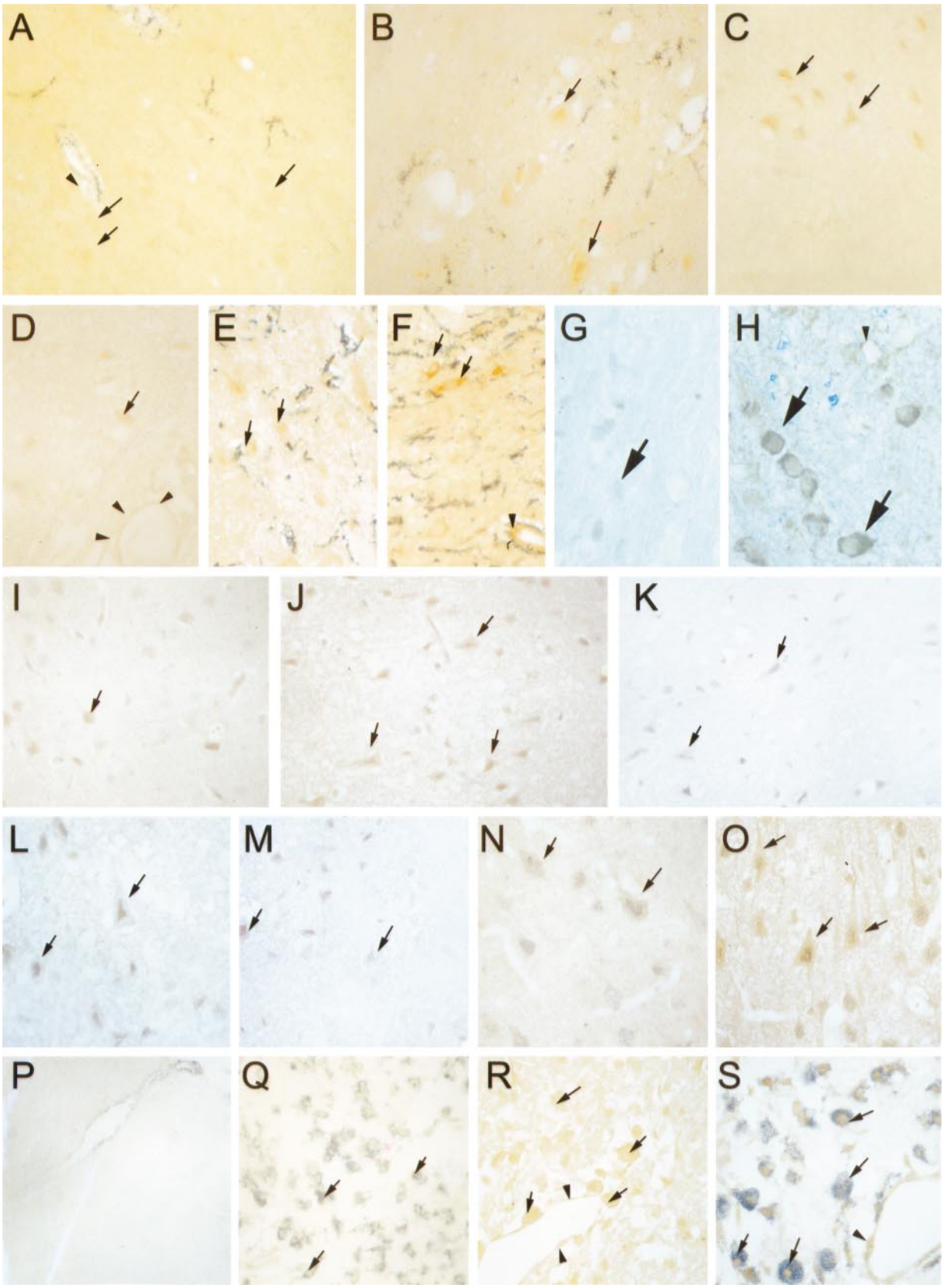

Fig. 2. MMP-3 is expressed in control neurons and, after ischemia/reperfusion, MMP-3 expression increases in ischemic neurons, oligodendrocytes, microvasculature, and reactive microglia, but it is not detected in astrocytes. The regions shown are in cortex (**A–C, I–S**), striatum (**D**), and corpus callosum (**E–H**) of control (**A, E, G, I, N, P**) and at 1 day (**B–D, F, J–M, O**)

SN-agrin is cell-associated since it is a type-II transmembrane protein with an intracellular N-terminus and an extracellular C-terminus (22). The N-terminus can externalize cytosolic proteins and might serve as an association domain (27). The antibody that we used in the present study against rat agrin recognizes an epitope located close to the C-terminus of agrin forms containing the 8aa, 11aa, or 19aa insert at splicing site Z; these forms are restricted to the CNS (44). Here we show that C-terminal fragments of cleaved agrin after ischemia do not remain associated with the membrane. Whether this has a functional implication other than loss of neuronal membrane agrin remains to be seen. Proteolytic cleavage through ectodomain shedding, resulting from the action of MMP-3, might represent a regulatory control of agrin function in the CNS (27). The fact that agrin is a transmembrane protein in the CNS suggests that it acts as a receptor that mediates the translocation of signals from the extracellular space to the cytoplasm (22). In CNS neurons, agrin signals through synaptic receptors (42) that have been identified as integrins (27). Agrin regulates synapse differentiation in hippocampal neurons (43, 44) and a role in regulating activity-dependent changes in synaptic efficacy has been proposed (45). A decrease in the number of differentiated synapses and defective synaptic transmission has been found in the superior cervical ganglion deficient in agrin (46). Furthermore, agrin-deficient neurons and mice are resistant to excitotoxic injury, thus suggesting that agrin is involved in glutamatergic transmission and in neuronal Ca^{2+} homeostasis (28). Therefore, loss of agrin from cell membranes in ischemia might contribute to impaired synaptic transmission, but it might confer resistance to excitotoxicity. Nevertheless, the fate and function of the cleaved C-terminal fragments remain unknown. C-terminal brain agrin fragments are able to induce CREB phosphorylation and c-*fos* expression, and several lines of evidence suggest that they bind to a discrete neuronal receptor at the synapses (26). According to this view, C-terminal agrin fragments that are released to the extracellular space in ischemia might stimulate neuronal Ca^{2+} influx and exacerbate the excitotoxic cascade.

MMP-3 Is Not Present in Resting Brain Astrocytes, but Agrin Is Found in Reactive Astrocytes following Ischemia/Reperfusion

Agrin was not found in resident astrocytes of the control brain. However, by the time that the glial scar was formed at 4 days post-ischemia, we observed that the reactive astrocytes showed some immunoreactivity to agrin. It is likely that this new agrin location results from agrin synthesized de novo by reactive astrocytes, and it was found surrounding the cell body and processes, suggesting that it was the transmembrane form of agrin. Agrin expression was also detected in cultured astrocytes, which were studied at the time they reached confluence. These cultured astrocytes showed basal expression of 27-kDa heat-shock protein (34), which is not normally found in resident astrocytes of the control brain (47), suggesting that they have some degree of reactivity. It is conceivable that agrin in reactive astrocytes might contribute to astrocytic connection and communication and might be involved in the formation of a *non*permissive environment to axon growth, as the C-terminal fragment of agrin inhibits axon elongation (48). Agrin in reactive astrocytes would remain protected from proteolytic cleavage because these cells are devoid of MMP-3, offering an explanation of why it remained in the glial scar for several days.

MMP-3, but not Agrin, Is Expressed in Mature Oligodendrocytes and MMP-3 Expression Is Increased in Oligodendrocytes following Ischemia/Reperfusion

In contrast to astrocytes, oligodendrocytes were immunoreactive to MMP-3 in the corpus callossum of control brains. Following ischemia, the intensity of MMP-3

←

and 4 days (**H, Q–S**) post-ischemia. **A–F:** MMP-3 staining in brown does not colocalize with GFAP staining in dark blue. **A:** Low MMP-3 (brown) staining in control neurons (arrows), but not astrocytes (black) and vessels (arrowhead). **B, D:** In the zone surrounding the ischemic core the intensity of staining increases in neurons (arrows) and microvasculature (**D,** arrowheads). **C:** Neurons within the ischemic core show MMP-3 staining concentrated in their nuclei (arrows). **E:** MMP-3 stains oligodendrocytes (arrows) in the control corpus callosum, and (**F**) the intensity of staining increases following ischemia in these cells (arrows) and in vessels (arrowhead). **G, H:** MMP-3-stained oligodendrocytes are shown in brown and myelinated fibers are stained bright blue with Luxol fast blue; oligodendrocytes show a strong increase in MMP-3 staining 4 days post-ischemia (**H,** arrows) relative to controls (**G,** arrows). Blue staining patches in (**H**) indicate disrupted myelin fibers. **I–M:** Hematoxylin counterstained sections in the presence (**I, J, L**) or absence (**K, M**) of the primary antibody against MMP-3 in a section from a control rat (**I**) and in sections from ischemic rats (**J–M**). **N, O:** Double immunohistochemistry against MMP-3 (brown) and the NeuN neuronal marker (black) in control (**N**) and ischemic (**O**) cortex. Ischemic, shrunken neurons showing triangular morphology are apparent in (**J–M**) and (**O,** arrows). **P–S**: Staining of MMP-3 (brown) and lectin (dark blue), a marker of microglia/macrophages, shows colocalization (**S**) at 4 days post-ischemia. **P:** No cellular staining is detected in the control cortex, but MMP-3-labeled reactive microglia/macrophages (**S**, arrows) are apparent 4 days post-ischemia. Immunoreaction controls include (**Q**) omission of the primary antibody against MMP-3 (revealing reactive microglia/macrophages stained in black, arrows), and (**R**) omission of lectin (evidencing MMP-3 stained cells with the morphology of reactive microglia/macrophages, arrows). Bar scale: G–H = 15 μm; A–F, L–S = 25 μm; I–K = 50 μm.

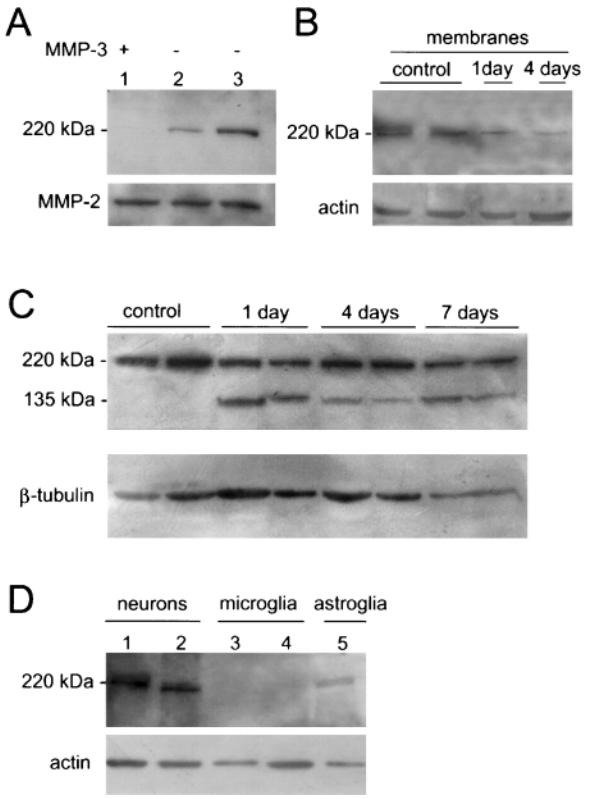

Fig. 3. MMP-3 degrades transmembrane neuronal agrin, which becomes cleaved following ischemia, concomitant with MMP-3 activation. **A:** Homogenates of control brain tissue (from rats not subjected to ischemia) were incubated in the presence (lane 1) or absence (lanes 2, 3) of 1.6 U of human recombinant MMP-3 per μg of tissue protein. Samples in lanes 1 and 2 were incubated at 37°C in MMP-3 buffer (see Materials and Methods) for 18 hours, whereas the sample in lane 3 was directly loaded on the gel without prior incubation. MMP-2 expression in the same gel is shown to illustrate equal protein loading in each lane. MMP-3 has the ability to degrade brain agrin. **B:** Isolated membrane preparations from brain tissue of controls or brains obtained at 1 and 4 days post-ischemia show reduced transmembrane agrin expression following ischemia. Actin is shown at the bottom as a protein loading control. **C**: In homogenates of brain tissue from controls and at 1, 4, and 7 days post-ischemia the reduction of 220-kDa transmembrane agrin is accompanied by the formation of a 135-kDa agrin-cleaved fragment containing the C-terminal region, where the recognition epitope for the antibody used is located. β-tubulin is shown as a control for protein loading in the different lanes. **D:** In cultured cells, transmembrane agrin is detected in neurons and to a much lesser extent in astrocytes, but not in microglia. Actin is shown as a protein loading control.

staining was markedly increased in oligodendrocytes located in the ischemic area, including those in the ipsilateral corpus callossum and also in the cortex and striatum in the vicinity of, and within, the glial scar. In the injured CNS, oligodendrocytes become reactive; they show signs of hypertrophy, they divide, and then differentiate to provide new oligodendrocytes for re-myelination (49). MMP-3 expression correlates with the invasive properties of human astrocytoma cell lines due to the proteolytic effects of MMP-3 on extracellular matrix macromolecules (2). Although oligodendrocytes might use MMP-3 to migrate within the parenchyma, we did not find MMP-3 in precursor oligodendrocytes. Lack of MMP-3 in oligodendrocyte precursors implies that these cells would be unable to degrade agrin, which might underlie the observation that astrocytes at the glial scar inhibit the migration of oligodendrocyte precursors (50). No expression of agrin was detected in oligodendrocytes in the tissue or in cultured cells.

Reactive Microglia/Macrophages Express MMP-3 and Contain Agrin Deposits

In addition to neurons and oligodendrocytes, some expression of MMP-3 was also detected in reactive microglia/macrophages following ischemia/reperfusion, in agreement with a previous report (5). These latter cells are located within the core of the infarction, where discrete deposits that were immunoreactive to agrin were observed surrounding blood vessels and within the infarcted parenchyma. Thus, these macrophage cells might remove matrix agrin accumulations within the infarcted regions. Accumulation of Luxol fast blue reactive material was also observed in reactive microglia/macrophages, which is compatible with myelin degradation. Myelin is also a substrate for MMP-3 (12), so it is likely that macrophage-associated MMP-3 contributes to agrin and myelin degradation by these cells.

Agrin and MMP-3 in the Microvasculature

Agrin is a component of the basal lamina (51–53), which is a specialized extracellular matrix structure that gives structural support to the microvasculature and in the brain has an essential role in maintaining the integrity of the blood-brain barrier (BBB). Following ischemia, the BBB breaks down and there is extravasation of plasma proteins to the parenchyma, with a maximum leakage by 1 to 2 days. In agreement with a previous report (5), we detected MMP-3 surrounding blood vessels after ischemia, which again might be responsible for agrin degradation at this location and thus contribute to increased BBB permeability. However, we did not observe agrin staining in the cerebral microvasculature since our antibody was specific to the neuronal form of agrin, whereas the form of agrin surrounding the microvasculature lacks the inserts at splicing site Z (54). Nevertheless, by 4 to 7 days after ischemia we detected strong agrin-immunoreactive deposits surrounding the blood vessels within the infarct, suggesting that certain neuronal agrin fragments formed after ischemia accumulated at this site.

In summary, this study shows 1) the activation of MMP-3 in ischemia/reperfusion, where it was found in

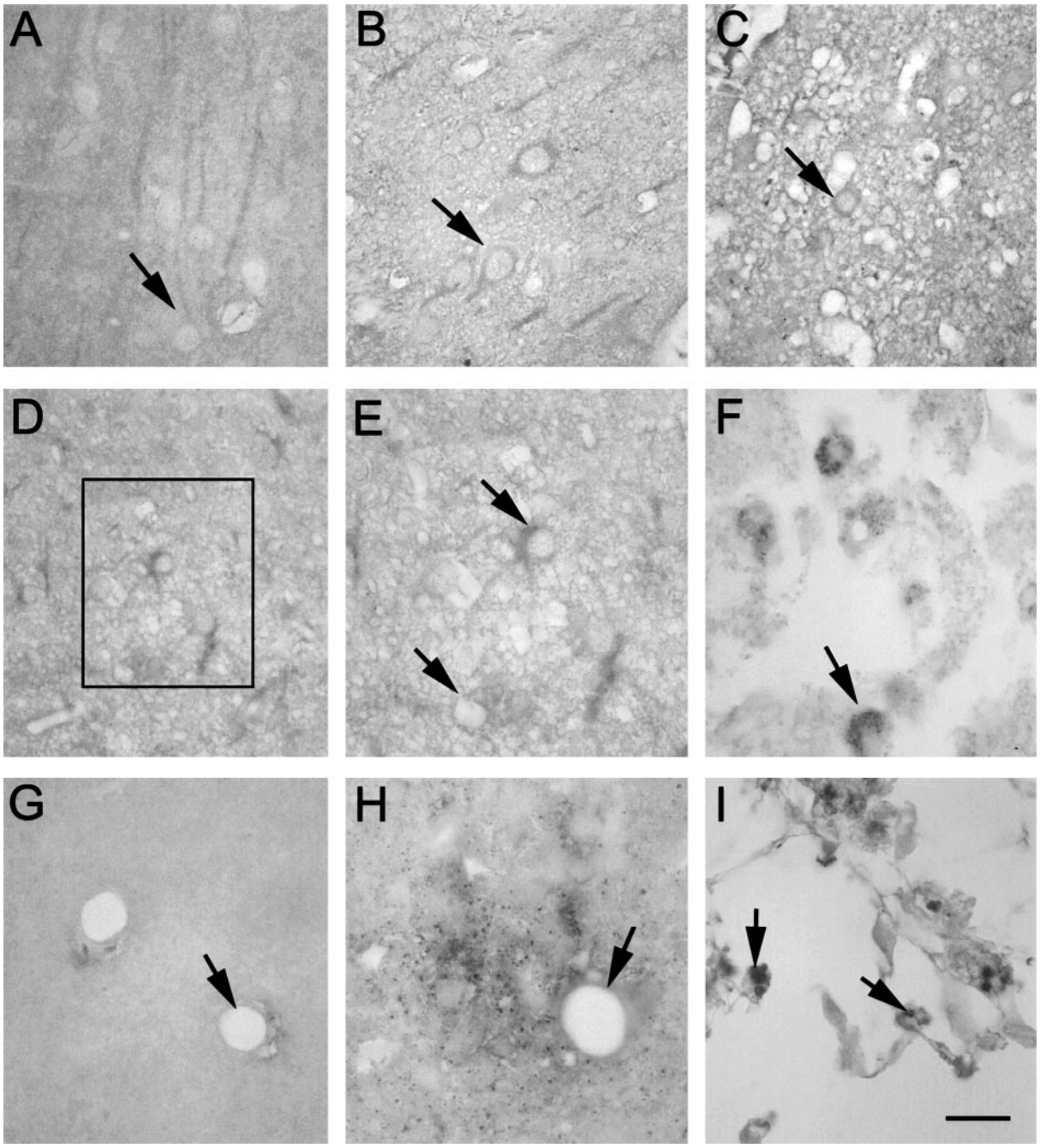

Fig. 4. Ischemia induces loss of neuronal transmembrane agrin, expression of transmembrane agrin in reactive astrocytes, and agrin deposits in microglia/macrophages and surrounding microvessels. **A:** Transmembrane agrin is detected in neurons (arrow) of the control cortex surrounding the cell bodies and cell processes, in rats not subjected to ischemia, and in the contralateral hemisphere of ischemic rats. **B:** At 24 hours following ischemia/reperfusion, cortical neurons in the vicinity of the ischemic core show stronger staining around the cell body (arrow) and discontinuous staining in neuronal processes, suggesting disturbances in axonal transport. **C:** Within the ischemic core, neuronal agrin staining is lost and only scattered immunoreactive neurons (arrow) are seen. **D:** Reactive astrocytes in the glial scar become immunoreactive to agrin. The area marked in the square is magnified in (**E**). **E:** Agrin staining in reactive astrocytes (arrows) is seen surrounding the cell body and processes at 4 days after the onset of ischemia. **F:** At 4 days, reactive microglia/macrophages in the infarcted area show agrin deposits, which become more marked at 14 days (**I**). **G:** Brain agrin is not found in the microvasculature (arrow) of control brains, but agrin deposits surrounding blood vessels (arrow) become apparent from 4 days post-ischemia (**H**). Control brain = **A, D, G**; 1-day post-ischemia = **B, C**; 4-day post-ischemia = **F–H**; 14-day post-ischemia = **D, E, I**. Bar scale: A–D = 20 μm, E–I = 12 μm.

neurons, oligodendrocytes, and reactive microglia/macrophages; 2) the ability of MMP-3 to cleave neuronal brain agrin; 3) the disappearance of neuronal membrane agrin following ischemia, with the generation of cleaved agrin fragments that did not remain associated with cell membranes; and 4) agrin expression by reactive astrocytes. These results support the view that ischemia/reperfusion causes MMP-3 activation, resulting in the cleavage of certain proteins such as agrin and myelin. This study also suggests that transmembrane neuronal agrin cleavage might impair synaptic neurotransmission and enhance excitotoxicity through the action of released C-terminal agrin fragments, and that agrin expression by reactive astrocytes might contribute to the generation of a *non*permissive environment for axon growth.

ACKNOWLEDGMENTS

We thank Dr. Eduardo Molina-Holgado for providing cultured oligodendrocytes. S. Solé and R. Gorina were recipients of fellowships from IDIBAPS, and Dr. V. Petegnief was supported by the MCYT. We wish to thank Mr. Robin Rycroft for editorial assistance.

REFERENCES

1. Nagase H, Woessner JF Jr. Matrix metalloproteinases. J Biol Chem 1999;274:21491–94
2. Mercapide J, Lopez de Cicco R, Castresana JS, Klein-Szanto AJ. Stromelysin-1/matrix metalloproteinase-3 (MMP-3) expression accounts for invasive properties of human astrocytoma cell lines. Int J Cancer 2003;106:676–82
3. D'Souza CA, Mak B, Moscarello MA. The up-regulation of stromelysin-1 (MMP-3) in a spontaneously demyelinating transgenic mouse precedes onset of disease. J Biol Chem 2002;277:13589–96
4. Rosenberg GA, Sullivan N, Esiri MM. White matter damage is associated with matrix metalloproteinases in vascular dementia. Stroke 2001;32:1162–68
5. Rosenberg GA, Cunningham LA, Wallace J, et al. Immunohistochemistry of matrix metalloproteinases in reperfusion injury to rat brain: Activation of MMP-9 linked to stromelysin-1 and microglia in cell cultures. Brain Res 2001;893:104–12
6. Springman EB, Angleton EL, Birkedal-Hansen H, Van Wart HE. Multiple modes of activation of latent human fibroblast collagenase: Evidence for the role of a Cys73 active-site zinc complex in latency and a ''cysteine switch'' mechanism for activation. Proc Natl Acad Sci U S A 1990;87:364–68
7. Chen LC, Noelken ME, Nagase H. Disruption of the cysteine-75 and zinc ion coordination is not sufficient to activate the precursor of human matrix metalloproteinase 3 (stromelysin 1). Biochemistry 1993;32:10289–95
8. Murphy G, Cockett MI, Ward RV, Docherty AJ. Matrix metalloproteinase degradation of elastin, type IV collagen and proteoglycan. A quantitative comparison of the activities of 95 kDa and 72 kDa gelatinases, stromelysins-1 and -2 and punctuated metalloproteinase (PUMP). Biochem J 1991;277:277–79
9. Fosang AJ, Neame PJ, Hardingham TE, Murphy G, Hamilton JA. Cleavage of cartilage proteoglycan between G1 and G2 domains by stromelysins. J Biol Chem 1991;266:15579–82
10. Agnihotri R, Crawford HC, Haro H, Matrisian LM, Barda MC, Liaw L. Osteopontin, a novel substrate for matriz metalloproteinase-3 (Stromelysin-1) and matrix metalloproteinase-7 (Matrilysin). J Biol Chem 2001;276:28261–67
11. Sage EH, Reed M, Funk SE, et al. Cleavage of the matricellular protein SPARC by matrix metalloproteinase 3 produces polypeptides that influence angiogenesis. J Biol Chem 2003;278:37849–57
12. Chandler S, Coates R, Gearing A, Lury J, Wells G, Bone E. Matrix metalloproteinases degrade myelin basic protein. Neurosci Lett 1995;201:223–6
13. Gearing AJH, Thorpe SJ, Miller K, et al. Selective cleavage of human IgG by the matrix metalloproteinases, matrylisin and stromelysin. Immunol Lett 2002;81:41–48
14. Ramos-DeSimone N, Hahn-Dantonav E, Sipley J, Nagase H, French DL, Quigley JP. Activation of matrix metalloproteinase-9 (MMP-9) via a converging plasmin/stromelysin-1 cascade enhances tumor cell invasion. J Biol Chem 1999;274:13066–76
15. McQuibban GA, Gong J-H, Wong JP, Wallace JL, Clark-Lewis I, Overall CM. Matriz metalloproteinase processing of monocyte chemoattractant proteins generates CC chemokine receptor antagonists with anti-inflammatory properties in vivo. Blood 2002;100:1160–67
16. VanSaun M, Werle MJ. Matrix metalloproteinase-3 removes agrin from synaptic basal lamina. J Neurobiol 2000;43:140–49
17. Tsen G, Halfer W, Kroger S, Cole GJ. Agrin is a heparan sulfate proteoglycan. J Biol Chem 1995;270:3392–99
18. Reist NE, Magill C, McMahan UJ. Agrin-like molecules at synaptic sites in normal, denervated, and damaged skeletal muscles. J Cell Biol 1987;105:2457–69
19. Reist NE, Werle MJ, McMahan UJ. Agrin released by motor neurons induces the aggregation of acetylcholine receptors at neuromuscular junctions. Neuron 1992;8:865–68
20. Burgess RW, Skarnes WC, Sanes JR. Agrin isoforms with distinct amino termini: Differential expression, localization and function. J Cell Biol 2000;151:41–52
21. O'Connor LT, Lauterborn JC, Gall CM, Smith MA. Localization and alternative splicing of agrin mRNA in adult rat brain: Transcripts encoding isoforms that aggregate acetylcholine receptors are not restricted to cholinergic regions. J Neurosci 1994;14:1141–52
22. Neumann FR, Bittcher G, Annies M, Schumacher B, Kröger S, Ruegg MA. An alternative amino-terminus expressed in the central nervous system converts agrin to a type II transmembrane protein. Mol Cell Neurosci 2001;17:208–25
23. Kroger S, Mann S. Biochemical and functional characterization of basal lamina-bound agrin in the chick central nervous system. Eur J Neurosci 1996;8:500–509
24. Halfter W, Schurer B, Yip J, Yip L, Tsen G, Lee JA, Cole GJ. Distribution and substrate properties of agrin, a heparan sulfate proteoglycan of developing axonal pathways. J Comp Neurol 1997; 383:1–17
25. Koulen P, Honig LS, Fletcher EL, Kroger S. Expression, distribution and ultrastructural localization of the synapse-organizing molecule agrin in the mature avian retina. Eur J Neurosci 1999;11: 4188–96
26. Smith MA, Hilgenberg LGW. Agrin in the CNS: A protein in search of a function? NeuroReport 2002;13:485–95
27. Burgess RW, Dickman DK, Nunez L, Glass DJ, Sanes JR. Mapping sites responsible for interactions of agrin with neurons. J Neurochem 2002;83:271–84
28. Hilgenberg LGW, Ho KD, Lee D, O'Dowd DK, Smith MA. Agrin regulates neuronal responses to excitatory neurotransmitters in vitro and in vivo. Mol Cell Neurosci 2002;19:97–110
29. Witte OW, Bidmon HJ, Schiene K, Redecker C, Hagemann G. Functional differentiation of multiple perilesional zones after focal cerebral ischemia. J Cereb Blood Flow Metab 2000;20:1149–65
30. Lu A, Tang Y, Ran R, Clark JF, Aronow BJ, Sharp FR. Genomics of the periinfarction cortex after focal cerebral ischemia. J Cereb Blood Flow Metab 2003;23:786–810
31. Justicia C, Pérez-Asensio FJ, Burguete MC, Salom JB, Planas AM. Administration of transforming growth factor-α reduces infarct volume after transient focal cerebral ischemia in the rat. J Cereb Blood Flow Metab 2001;21:1097–1104

32. Soriano MA, Sanz O, Ferrer I, Planas AM. Cortical infarct volume is dependent on the ischemic reduction of perifocal cerebral blood flow in a three-vessel intraluminal MCA occlusion/reperfusion model in the rat. Brain Res 1997;747:273–78
33. Petegnief V, Friguls B, Sanfeliu C, Suñol C, Planas AM. Transforming growth factor-α attenuates NMDA toxicity in cortical cultures by preventing protein synthesis inhibition through an Erk1/2-dependent mechanism. J Biol Chem 2003;278:29552–59
34. Fauconneau B, Petegnief V, Sanfeliu C, Piriou A, Planas AM. Induction of heat shock proteins (HSPs) by sodium arsenite in cultured astrocytes and reduction of hydrogen peroxide-induced cell death. J Neurochem 2002;83:1338–48
35. Saura J, Petegnief V, Wu X, Liang Y, Paul SM. Microglial apolipoprotein E and astroglial apolipoprotein J expression *in vitro*: Opposite effects of lipopolysaccharide. J Neurochem 2003;85:1455–67
36. Molina-Holgado E, Khorchid A, Liu H-N, Almazan G. Regulation of muscarinic receptor function in developing oligodendrocytes by agonist exposure. Br J Pharmacology 2003;138:47–56
37. Planas AM, Justicia C, Soriano MA, Ferrer I. Epidermal growth factor receptor in proliferating reactive glia following transient focal ischemia in the rat brain. Glia 1998;23:120–29
38. Bickett DM, Green MD, Wagner C, Roth JT, Berman J, McGeehan GM. A high throughput fluorogenic substrate for stromelysin (MMP-3). Ann N Y Acad Sci 1994;732:351–55
39. Deb S, Gottschall PE. Increased production of matrix metalloproteinases in enriched astrocyte and mixed hippocampal cultures treated with beta-amyloid peptides. J Neurochem 1996;66:1641–47
40. Garcia JH, Yoshida Y, Chen H, Li Y, Zhang ZG, Lian J, Chen S, Chopp M. Progression from ischemic injury to infarct following middle cerebral artery occlusion in the rat. Am J Pathol 1993;142:623–35
41. Hoch W, Campanelli JT, Harrison S, Scheller RH. Structural domains of agrin required for clustering of nicotinic acetylcholine receptors. EMBO J 1994;13:2814–21
42. Hoover CL, Hilgenberg LGW, Smith MA. The COOH-terminal domain of agrin signals via a synaptic receptor in central nervous system neurons. J Cell Biol 2003;161:923–32
43. Böse CM, Qiu D, Bergamaschi A, et al. Agrin controls synaptic differentiation in hippocampal neurons. J Neurosci 2000;20:9086–95
44. Ferreira A. Abnormal synapse formation in agrin-depleted hippocampal neurons. J Cell Sci 1999;112:4729–38
45. Lesuisse C, Qiu D, Böse CM, Nakaso K, Rupp F. Regulation of agrin expression in hippocampal neurons by cell contact and electrical activity. Mol Brain Res 2000;81:92–100
46. Gingras J, Rassadi S, Cooper E, Ferns M. Agrin plays an organazing role in the formation of sympathetic synapses. J Cell Biol 2002;158:1109–18
47. Kato H, Araki T, Itoyama Y, Kogure K, Kato K. An immunohistochemical study of heat shock protein-27 in the hippocampus in a gerbil model of cerebral ischemia and ischemic tolerance. Neuroscience 1995;68:65–71
48. Mantych KB, Ferreira A. Agrin differentially regulates the rates of axonal and dendritic elongation in cultured hippocampal neurons. J Neurosci 2001;21:6802–9
49. Levine JM, Reynolds R, Fawcett JW. The oligodendrocyte precursor cell in health and disease. Trends in Neurosci 2001;24:39–47
50. Fawcett JW, Asher RA. The glial scar and the central nervous system. Brain Res Bull 1999;49:277–91
51. Rupp F, Payan DG, Magill-Solc C, Cowan DM, Scheller RH. Structure and expression of a rat agrin. Neuron 1991;6:811–23
52. Magill-Solc C, McMahan UJ. Motor neurons contain agrin-like molecules. J Cell Biol 1988;107:1825–33
53. Godfrey EW. Comparison of agrin-like proteins from the extracellular matrix of chicken kidney and muscle with neural agrin, a synapse organizing protein. Exp Cell Res 1991;195:99–109
54. Stone D, Nikolics K. Tissue- and age-specific expression patterns of alternatively spliced agrin mRNA transcripts in embryonic rat suggest novel developmental roles. J Neurosci 1995;15:6767–78

Received August 12, 2003
Revision received January 5, 2004
Accepted January 7, 2004